



# Weak lensing peak steepness statistics and Potential synergy of Euclid and CSST

**Zuhui Fan**  
**(SWIFAR, Yunnan University)**

Jan. 16, 2025

# Outline

- Introduction
- Weak lensing peak steepness statistics
- Potential synergy of Euclid and CSST
- Summary

# • Introduction

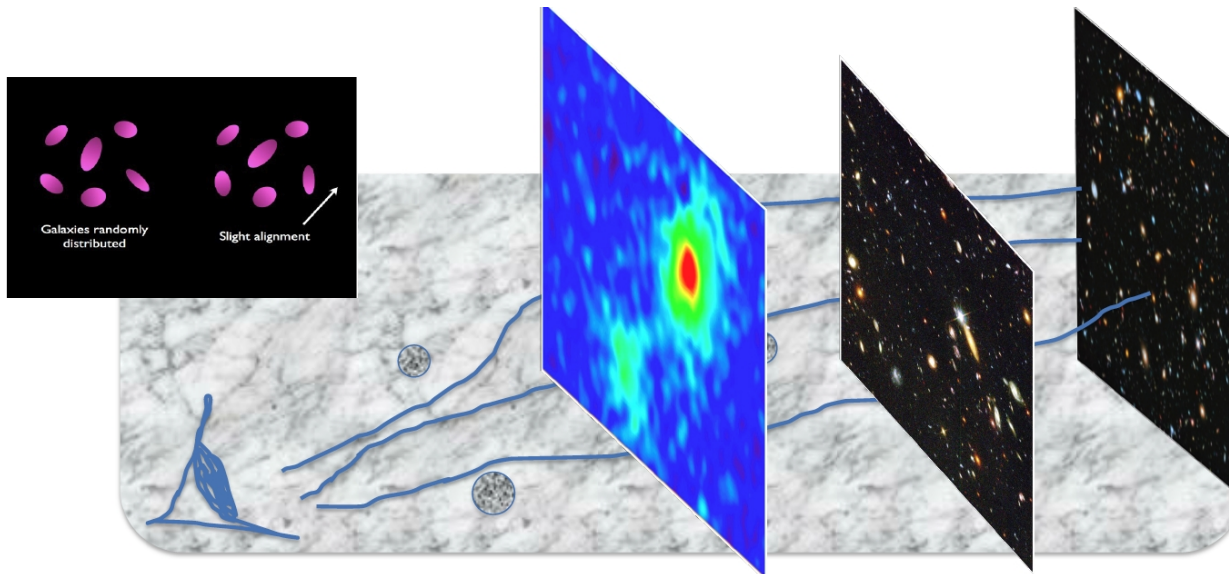
Among different probes, the weak lensing effect is uniquely important

Large-scale structures  $\rightarrow$  bend the light rays gravitationally

Observables: tiny shape distortion and flux change  $\rightarrow$  shear and magnification

Gravitational in origin  $\rightarrow$  unique probe to study the dark side of the universe  
dark matter and dark energy, law of gravity

Sensitive to both the cosmic expansion and the large scale structures



Weak lensing signals are weak → large sample to extract the correlated WL signals  
→ weak lensing cosmology → statistical in nature

Stage III surveys,  
DES, KIDS, HSC

- $\sim N^* 10^3 \text{ deg}^2$
- $\sim 10^{7-8}$  galaxies
- Deliver important cosmological constraints

Coming soon



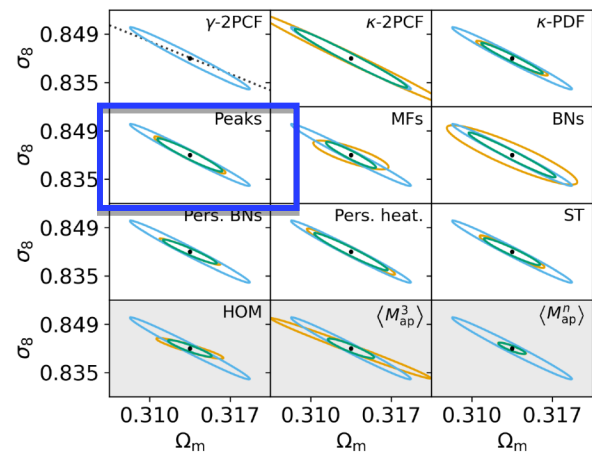
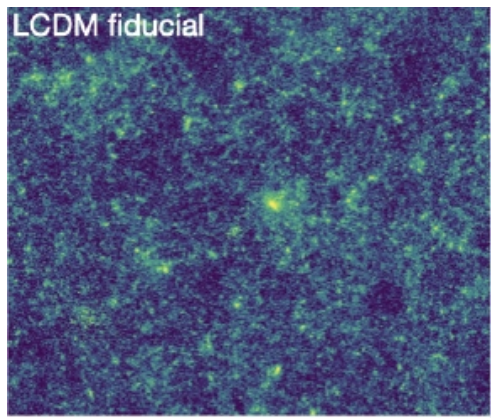
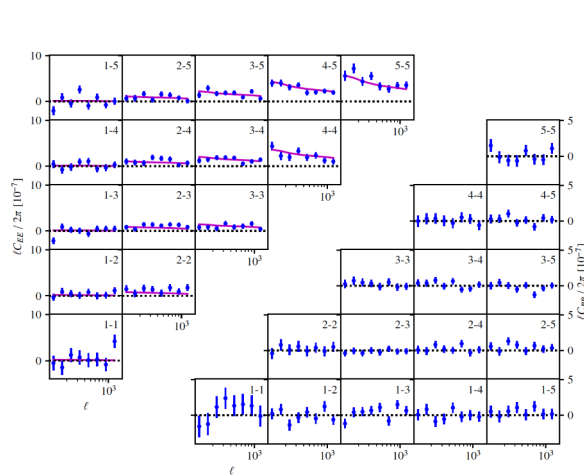
Stage IV surveys,  
Euclid, Roman, CSST  
LSST

- $\sim N^* 10^4 \text{ deg}^2$
- $\sim 10^9$  galaxies
- High precision cosmology

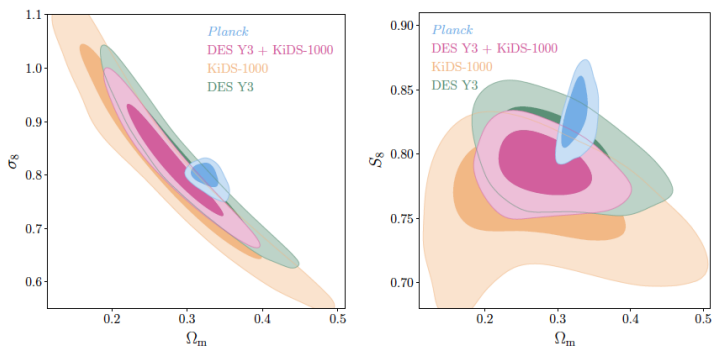


# Statistical analyses

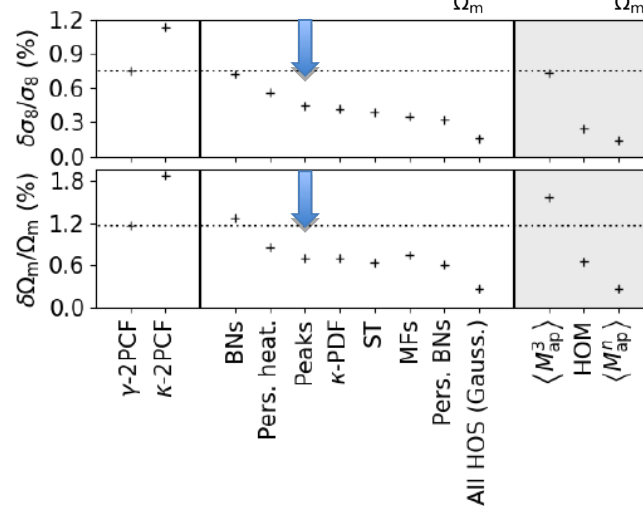
- **cosmic shear 2pt** is the primary statistics  
( 3×2pt: cosmic shear+ galaxy clustering +galaxy-galaxy lensing)
- **Density field is non-Gaussian**
- **Higher order non-Gaussian statistics are needed**



Heymans et al. 2021 (KiDS 1000)



Abbott et al. 2023, DES Y3+KiDS-1000



Euclid Collaboration HOWLS team et al. 2023

# Weak lensing peak statistics

LOS matter concentrations ( $\times$ lensing efficiency)  $\rightarrow$  high WL signals  $\rightarrow$  peaks in the WL mass maps  $\rightarrow$  nonlinear and non-Gaussian features  $\rightarrow$  cosmological inferences

To predict the cosmological dependences

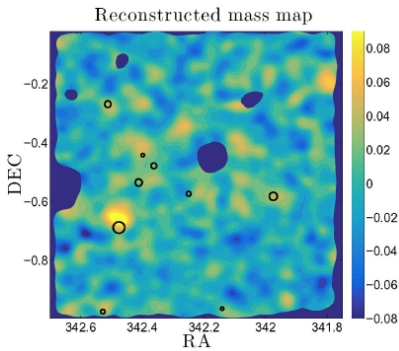
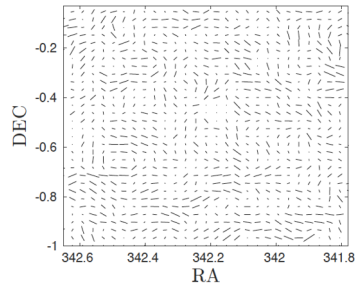


Run large sets of simulations to build numerical templates

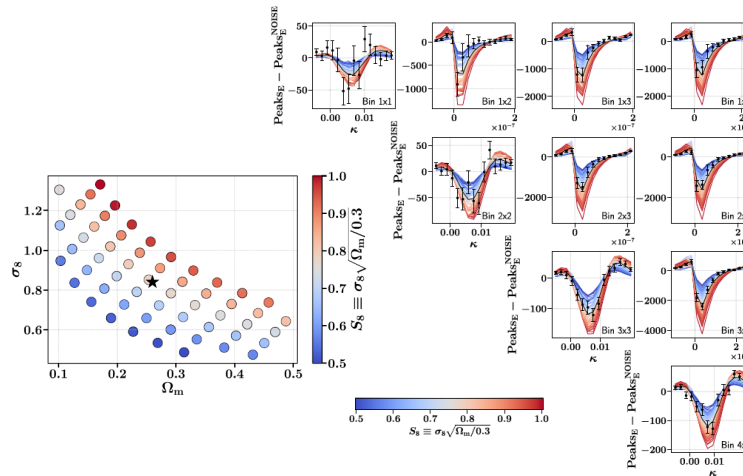


Incorporate theoretical modeling – our approach  
-- valid for high peaks

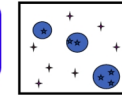
e.g., Zurcher et al. 2022, DES Y3



Liu, X. et al. 2015

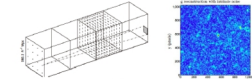


Model building  
-- predicting peak abundances given a cosmological model



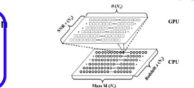
Halo model for high peaks taking into account the shape noise effect+LSS projection – crucial for cosmological studies with WL peaks (Fan et al. 2010, Yuan et al. 2018, Shan et al. 2018, ...)

Large sets of ray-tracing simulation



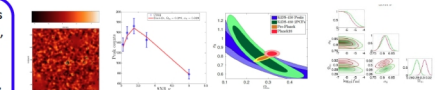
Mock simulation validation

Set up fast computation code for cosmological analyses

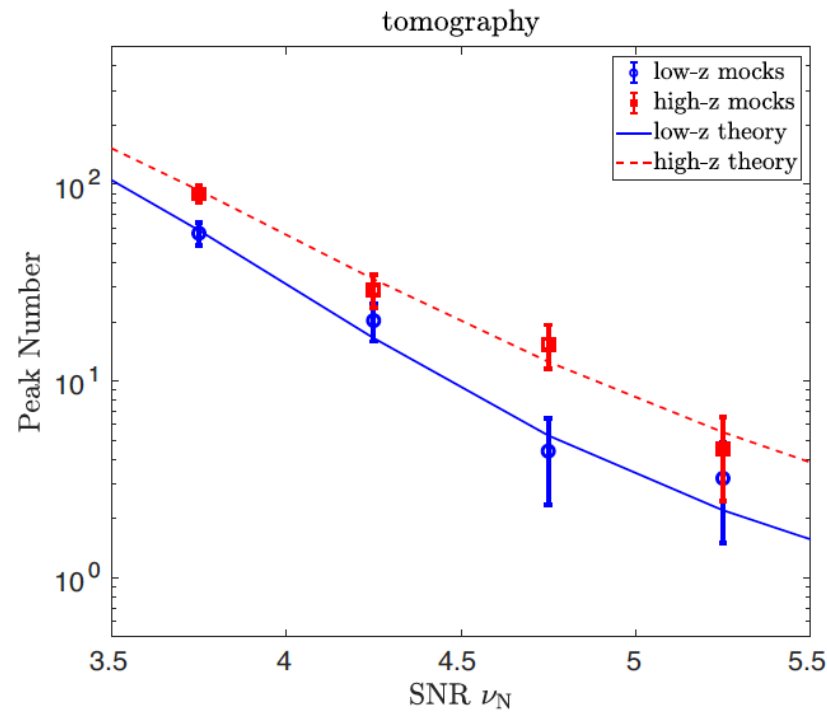
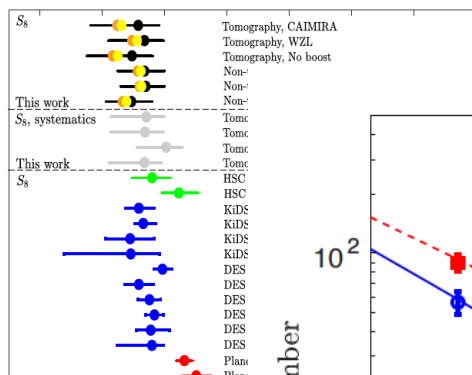
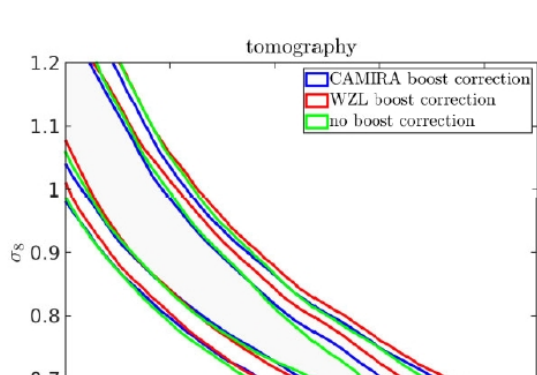


Cosmological constraints

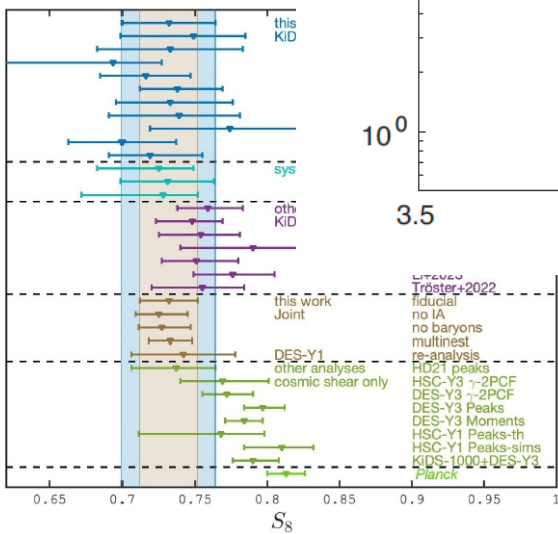
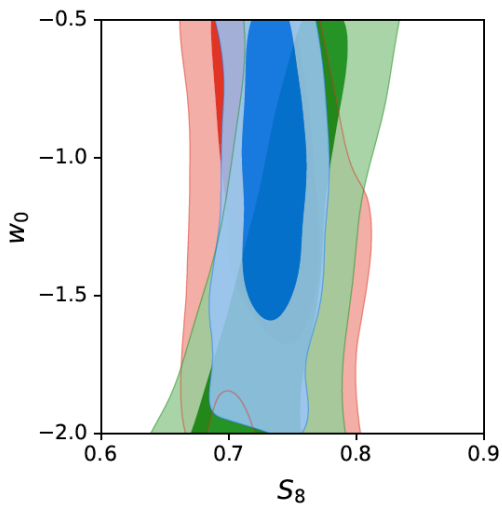
Observational analyses (CFHT CS82, CFHTLenS, KIDS, HSC,...) (Liu et al., 2015, 2016, 2023; Shan et al. 2018, Li et al. 2023)



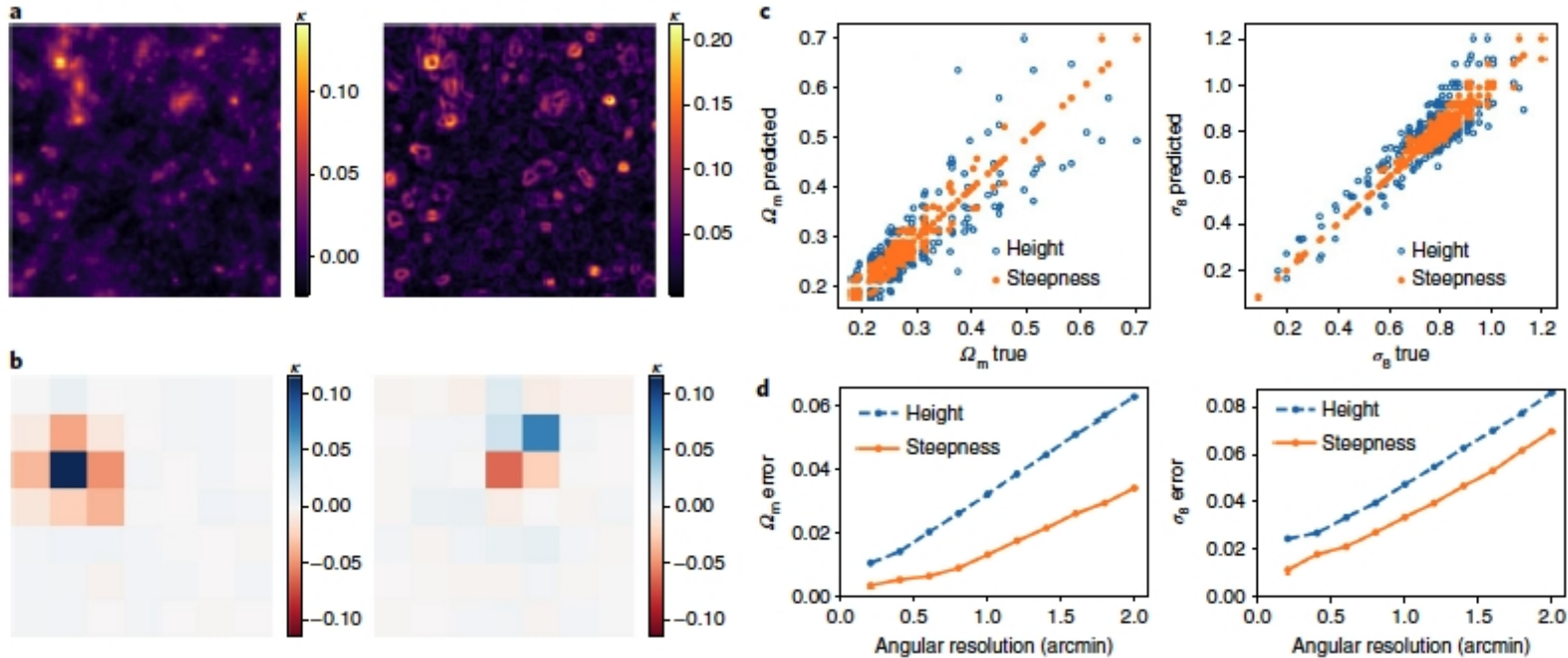
Peak statistics have been applied to different surveys (e.g., Liu,X. et al. 2015, Liu,J. et al. 2015, Liu, X. et al. 2016, Kacprzak et al. 2016, Martinet et al. 2018, Shan et al. 2018, Zurcher et al. 2022, Liu,X. et al. 2023, Harnois-Deraps et al. 2024)



All the peak analyses are in terms of peak height distribution



With deep learning, in Ribli et al. 2019, they analyzed the WL convergence map features, and found that the statistics of steepness (profile) of WL peaks carry additional cosmological information in comparison with the peak height statistics



Laplace operator

$$L_1 = \frac{-10}{3} \begin{bmatrix} -0.05 & -0.2 & -0.05 \\ -0.2 & 1 & -0.2 \\ -0.05 & -0.2 & -0.05 \end{bmatrix},$$

$$L_2 = -4 \begin{bmatrix} 0 & -0.25 & 0 \\ -0.25 & 1 & -0.25 \\ 0 & -0.25 & 0 \end{bmatrix}$$

Roberts cross kernels

$$R_x = \begin{bmatrix} 0 & 1 \\ -1 & 0 \end{bmatrix},$$

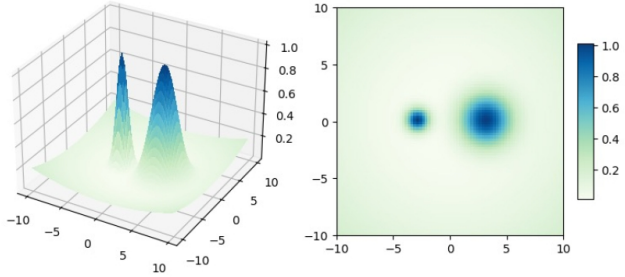
$$R_y = \begin{bmatrix} 1 & 0 \\ 0 & -1 \end{bmatrix},$$

$$G = \sqrt{G_x^2 + G_y^2},$$

Laplace operator  $\rightarrow$  second derivative  
 Roberts cross kernels  $\rightarrow$  first derivative



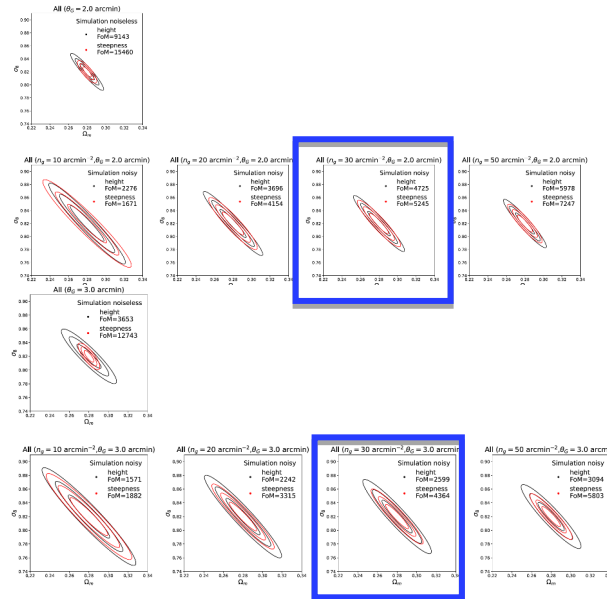
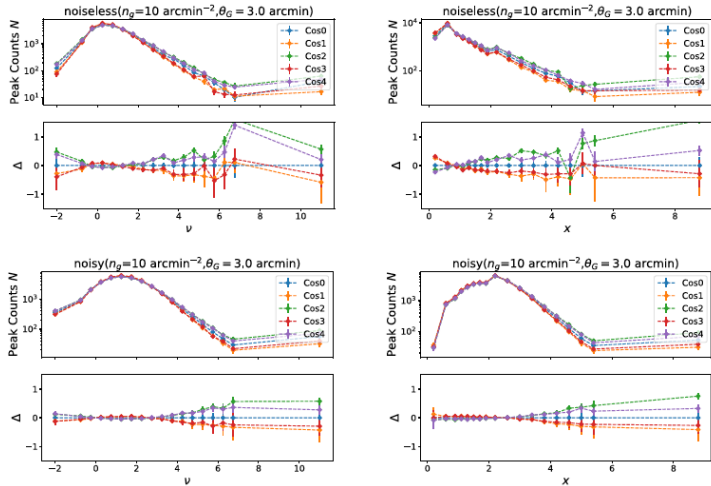
# ➤ WL peak steepness statistics (Li,Z.W. et al. 2023, 2025)



Mathematically, for a peak, its first derivatives are zero by definition. The steepness of a peak is reflected by its second derivatives

$$L_2 = -4 \begin{bmatrix} 0 & -0.25 & 0 \\ -0.25 & 1 & -0.25 \\ 0 & -0.25 & 0 \end{bmatrix} \longrightarrow \partial_{11}K + \partial_{22}K$$

With ray-tracing simulations, we perform analyses to compare the two statistics systematically -- different noise levels and smoothing scales  
 In the Stage IV era → peak steepness statistics can indeed give better cosmological constraints



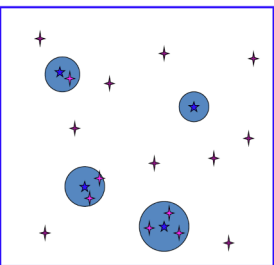
To understand the differences between the two statistics, we extended our halo-based model for high peaks (Fan,Z.H. et al. 2010, Yuan,S. et al. 2018) to the steepness statistics ( Li,Z.W. et al. 2023)

Assumption: Single massive halos contribute dominantly to WL peaks ( $M \geq M_* \sim 10^{14} h^{-1} M_{\text{sun}}$ )

→ valid for high peaks – **theoretically similar to cluster abundance, but different observables without the need to calibrate the mass-observable relation**

Including the shape noise and the LSS projection effects

→ adopt Gaussian approximation → **forward modelling approach**



$$\mathcal{K} = \mathcal{K}_H + \mathcal{K}_{\text{LSS}} + \mathcal{N}$$

$$n_{\text{peak}}(y)dy = \left[ n_{\text{peak}}^H(y) + n_{\text{peak}}^N(y) \right] dy$$

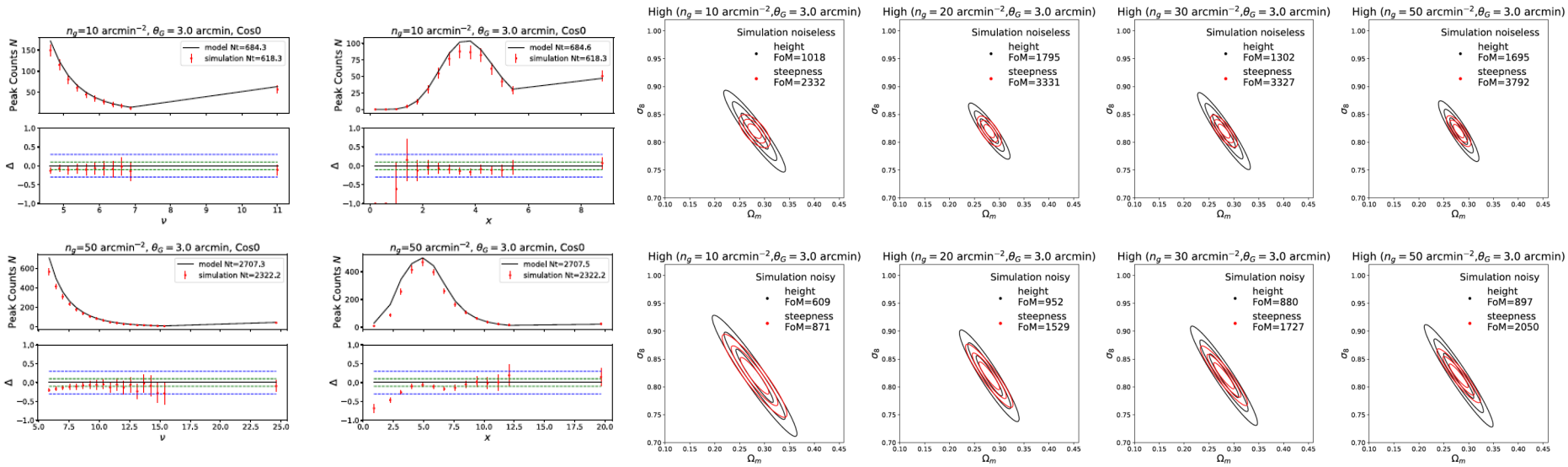
$$\begin{aligned} \hat{n}_{\text{peak}}(v_N) &= \exp \left[ -\frac{(K_H^1)^2 + (K_H^2)^2}{\sigma_1^2} \right] \left\{ \frac{1}{2\pi\theta_{N*}^2} \frac{1}{(2\pi)^{1/2}} \right\} \\ &\times \exp \left( -\frac{1}{2}u(v_N)^2 \right) dv_N \int_0^\infty \frac{dx_N}{[2\pi(1-\gamma_N^2)]^{1/2}} \\ &\times \exp \left[ -\frac{(m(x_N) - \gamma_N u(v_N))^2}{2(1-\gamma_N^2)} \right] \times F(x_N) \end{aligned}$$

$$\begin{aligned} \hat{n}_{\text{peak}}(x_N) \Big|_{v_N \geq v_{\text{cut}}} &= \exp \left[ -\frac{(K_H^1)^2 + (K_H^2)^2}{\sigma_1^2} \right] \left\{ \frac{1}{(2\pi\theta_{N*}^2)^2} \frac{(2\pi)^{1/2}}{2} \right\} \\ &\times \exp \left( -\frac{1}{2}m(x_N)^2 \right) \times \text{erfc}(t(v_{\text{cut}}, x_N)) \\ &\times F(x_N) dx_N, \end{aligned}$$

Physical ingredients: HMF, density profile, geometric distances

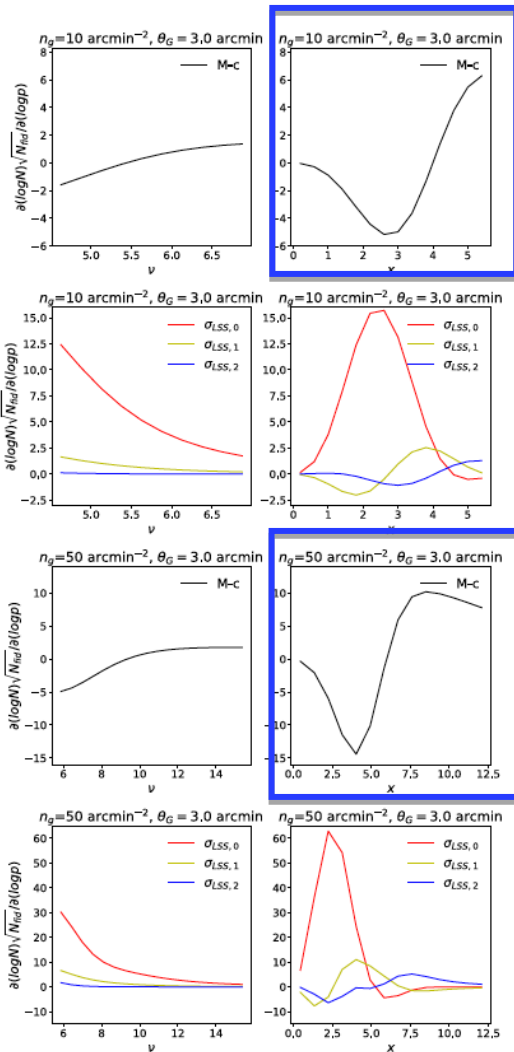
Incorporate systematics relatively straightforwardly: Baryonic effects → halo profile, HMF, LSS IA effects → lensing profile of clusters of galaxies, shape noise properties (Zhang et al. 2025)

# The model works well for both height and steepness statistics for high peaks



From the model, we can calculate the dependence of the two statistics on different physical parameters

# Different sensitivities to the physical parameters (from our model)



Steepness statistics:

$$c_{\text{vir}} = \frac{A}{(1+z)^{0.71}} \left( \frac{M_{\text{vir}}}{10^{14} h^{-1} M_{\odot}} \right)^{-0.081}$$

More sensitive to halo profile (M-c)

- M-c relation is mass and redshift dependent
- different weight on halo mass function

More sensitive to LSS projection effects (cosmological info.)

In addition to cosmological constraints, steepness statistics can probe **the density profile of halos**, which encodes information of

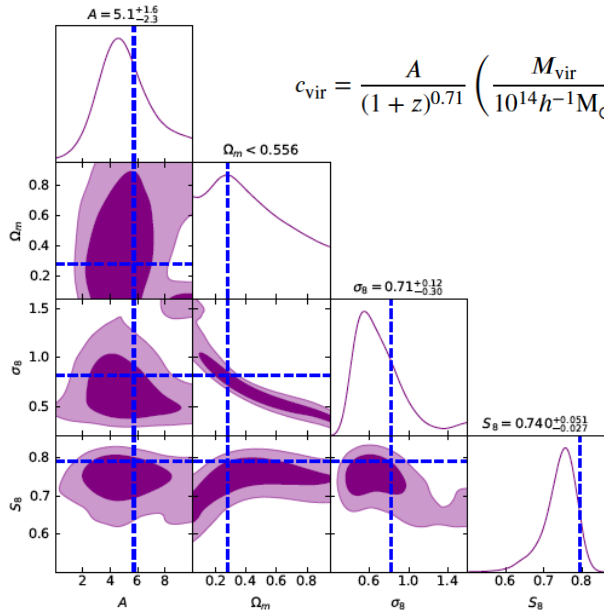
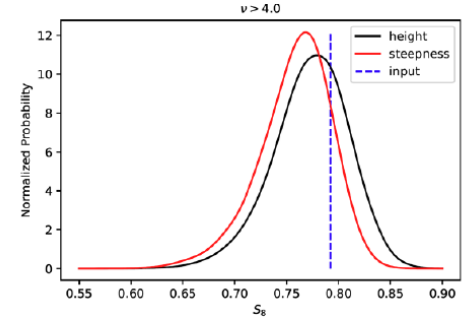
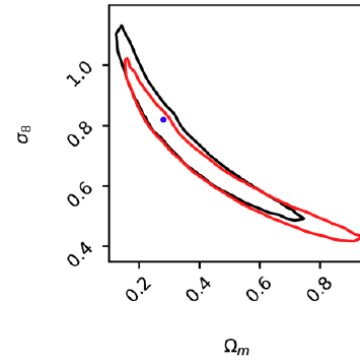
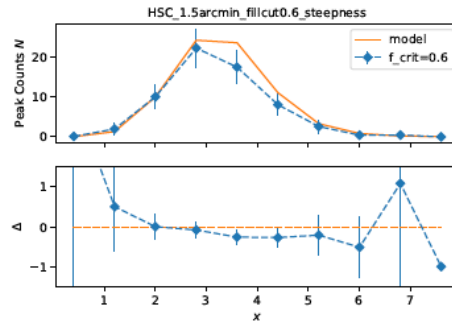
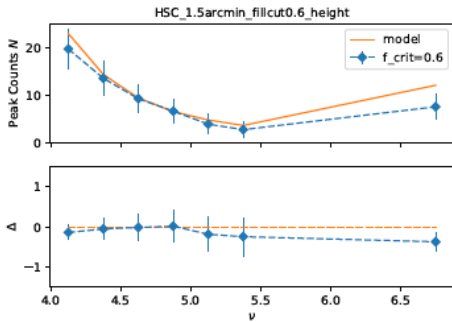
- **the baryonic effects**
- **dark matter properties**

→ **Unique advantage of peak steepness statistics**

# First application of the WL peak steepness analyses to HSC S16A data

(Li,Z.W. et al. 2025, in preparation)

Built mocks from N-body simulations with the same spatial and redshift distribution of sources – mask effects, convergence reconstruction, dark matter halo properties, MCMC pipeline



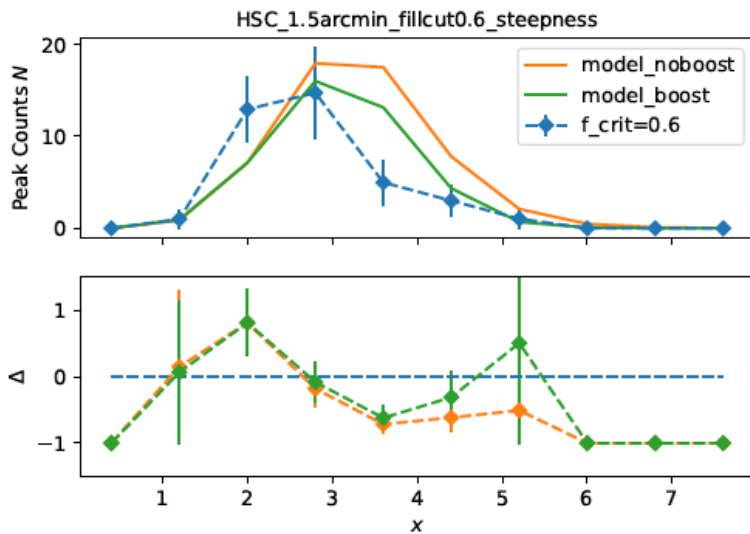
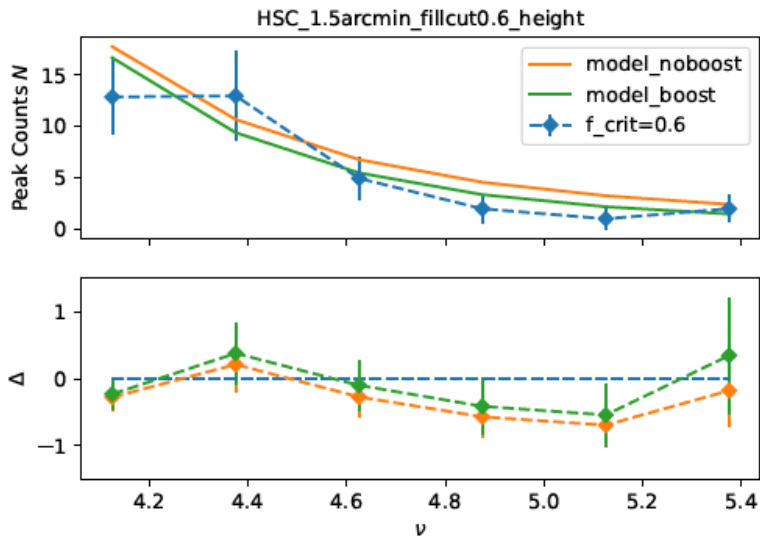
$$c_{\text{vir}} = \frac{A}{(1+z)^{0.71}} \left( \frac{M_{\text{vir}}}{10^{14} h^{-1} M_{\odot}} \right)^{-0.081}$$

By combining peak height and steepness analyses

→ Can indeed constrain M-c relation simultaneously with cosmological parameters

→ Potentially probe baryonic effects from WL-only observational data

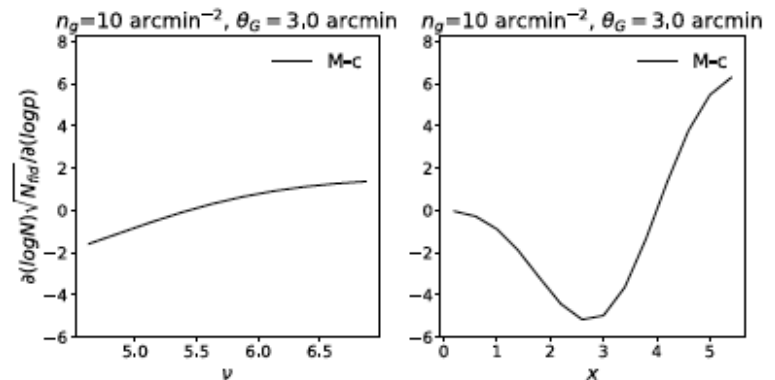
# Observational results from HSC-SSP S16A



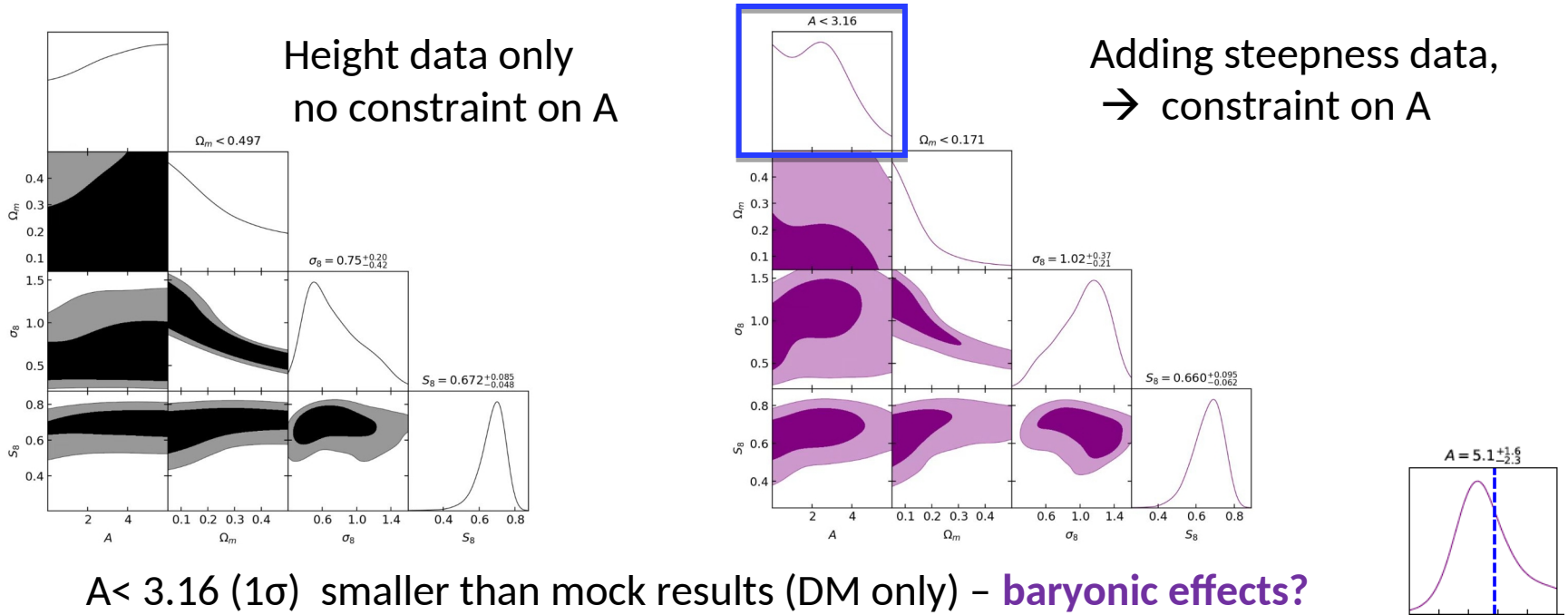
With dark matter only ingredients  
(M-c relation, HMF)

→ Steepness count distribution  
systematically shifts  
to lower values comparing to the  
model prediction that well fits the  
height distribution.

**Phenomenologically pointing to  
lower concentration**



# Observational results from HSC-SSP S16A (S/N>=4)

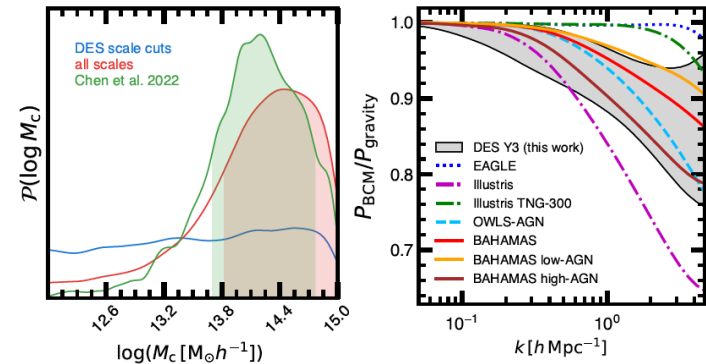
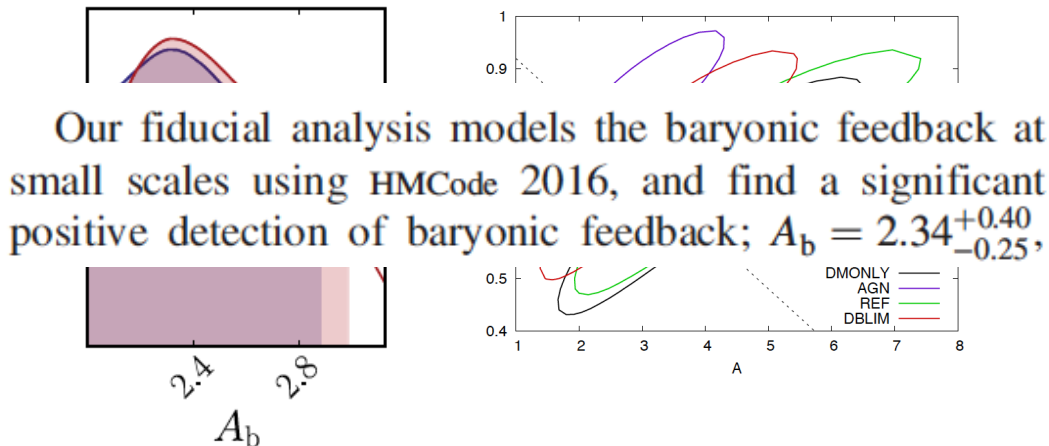


$A < 3.16$  ( $1\sigma$ ) smaller than mock results (DM only) – **baryonic effects?**

HSC Y3 3\*2pt (Li, X.C. et al. 2023)

Mead et al. 2015

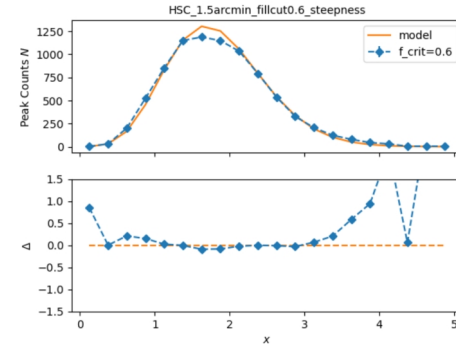
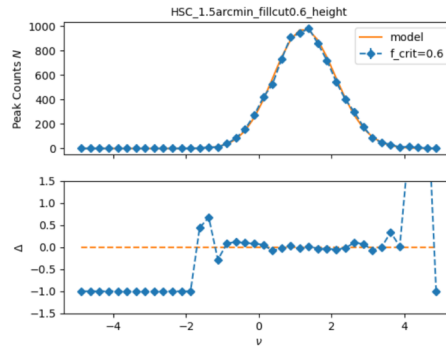
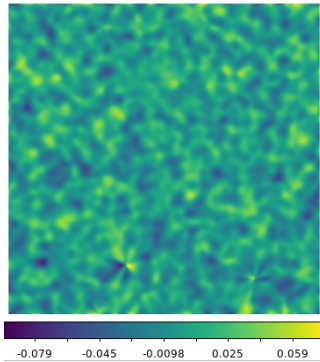
DES Y3 small-scale 2pt (Arico et al. 2023), BCM



# Before drawing conclusions, we did more tests on the data

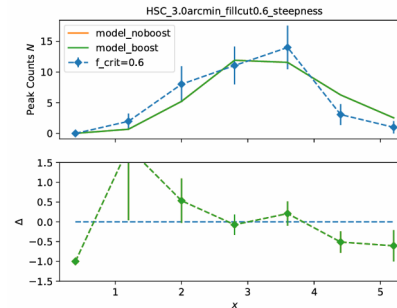
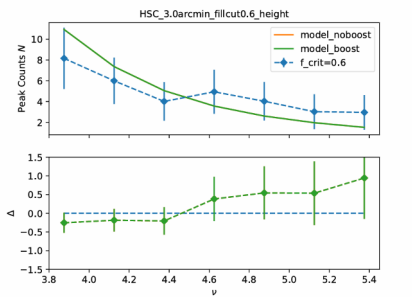
## -- B-mode test

peak height and steepness distributions are very much consistent with that of the pure Gaussian noise case (lines) – **No significant B-mode contaminations**



## -- Change the smooth scale from 1.5 arcmin to 3 arcmin

Convergence peaks – steepness distribution shows a similar trend as that of the case of 1.5 arcmin smoothing, although less significantly because of the fewer peaks and thus larger error bars





- ❖ Our current analyses: contribute all baryonic effects to halo profile (like HMcode 2016 for power spectrum) → pointing to positive baryonic effects
- ❖ We are further refining our model to predict the LSS projection effects consistently while changing the halo density profile (HMcode2016); also further checking the cluster member dilution effects
- ❖ Can also implement BCM into the model (dark matter+gas+stellar, change halo mass and profile)

### Take home message:

- **WL peak steepness analyses can provide sensitive constraints on halo profile → baryonic physics/dark matter properties**
- **shear accuracy requirements for Stage IV surveys**

For future high precision studies

- Requirement on the shear measurement accuracy from peak steepness statistics

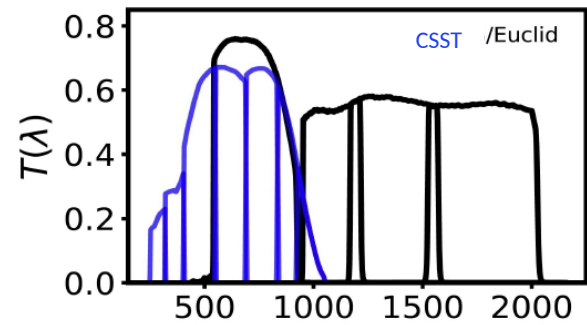
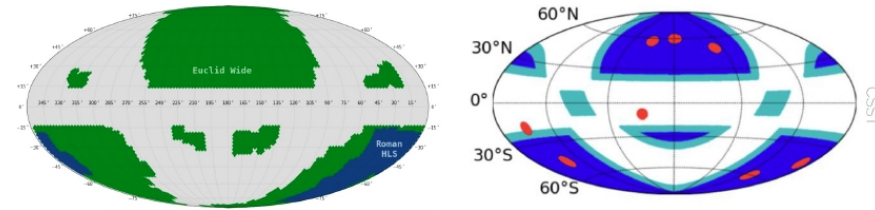
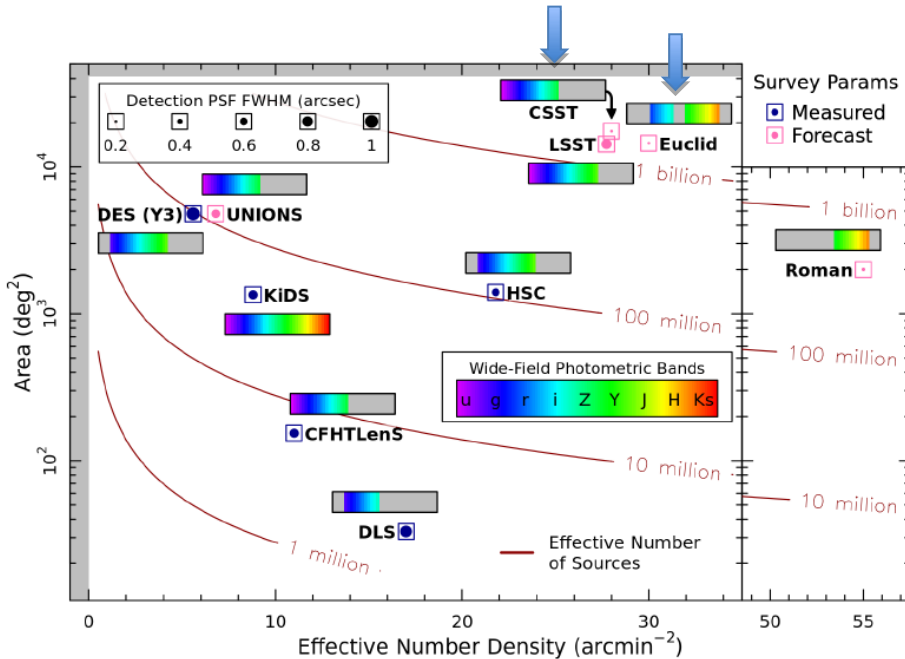
possible data problem: cluster regions are relatively crowded

- blending → shear measurement bias? → **advantage of CSST/Euclid**

# • Potential synergy of CSST and Euclid

Both China Space Station Survey Telescope (CSST) and Euclid of ESA are Stage IV surveys with the main scientific objectives to understand the nature of the dark components and inflationary physics.

**Similar spatial resolutions and nearly completely overlapped sky coverage.  
The filters are very complementary**



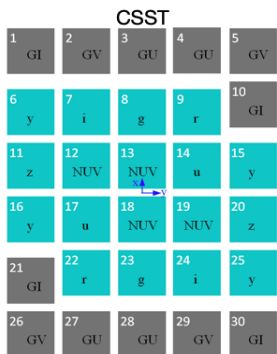
# Survey designs

>1 billion galaxies for weak lensing

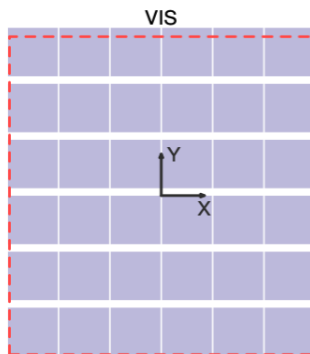
~100 million galaxies with spectral redshifts (Slitless spectral surveys)

Adapted from H.Zhan's slide

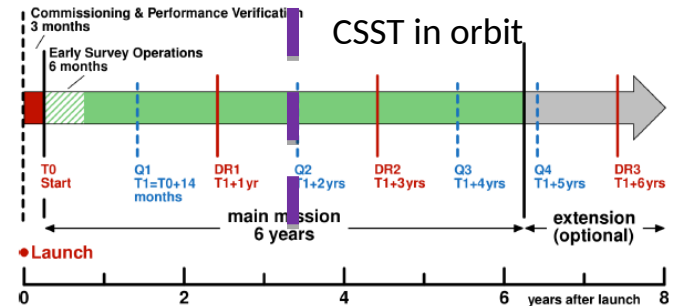
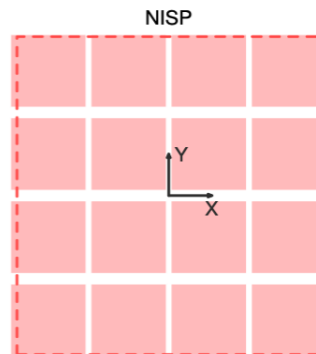
Project	Orbit/ Site	Launch/op	FoV	$R_{EE80}$	Num pixels	Area	Wavelength	Num filters	spectru m
			deg <sup>2</sup>	"	10 <sup>9</sup>	deg <sup>2</sup>	nm		
CSST 2m	LEO	~Mid 2027	1.1	0.15	2.5	17500	255—1000	7	Y
Euclid 1.2m	L2	July 1, 2023	0.56 0.55	0.2	0.6 0.07	15000	550—920 1000—2000	1 3	N Y
Roman Space Telescope RST 2.4m	L2	~ 2025	0.28	>0.2	0.3	2400	927—2000	4	Y
Rubin Observatory LSST 8.4m	Chile	~2025	9.6	~0.7	3.2	18000	320—1050	6	N



CSST



Euclid



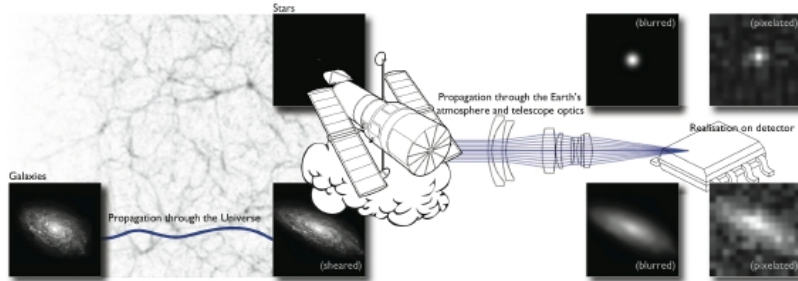
Euclid. I. Overview of Euclid mission 2024

For weak lensing studies:

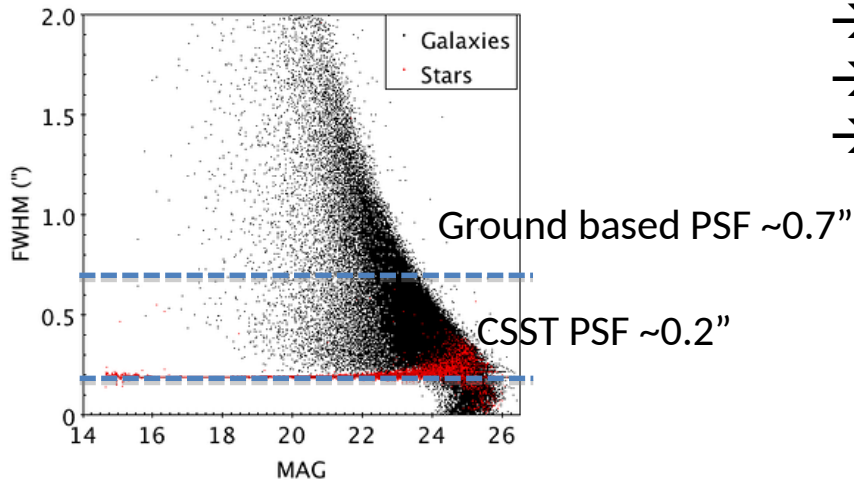
-- measure the shape of far-away galaxies accurately

-- measure their redshift with multi-band photometry → photo-z

## Shape measurement



## Galaxy size distribution



Space mission

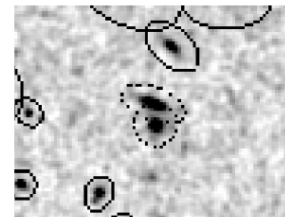
→ high resolution

→ Resolve smaller galaxies

→ Better measurements of shape and flux

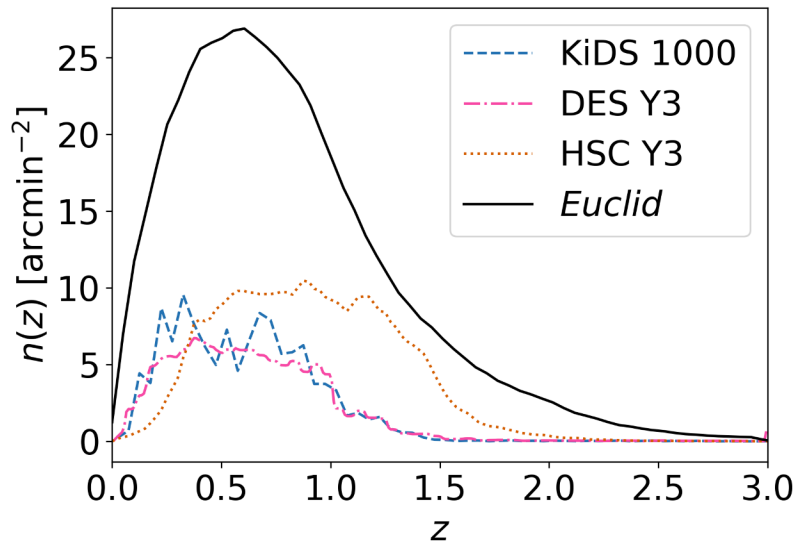
CSST/Euclid

ground  $\sim 0.7''$

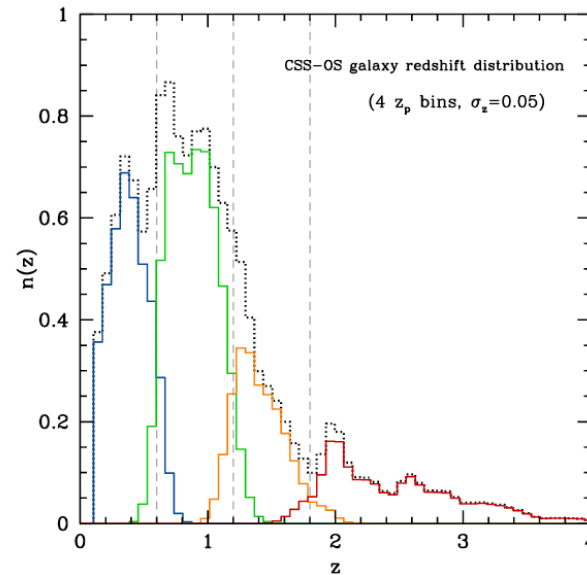


Accurate photo-z measurement is another important requirement in WL cosmology -- tomographic WL analyses

Expected Euclid and CSST galaxy redshift distribution



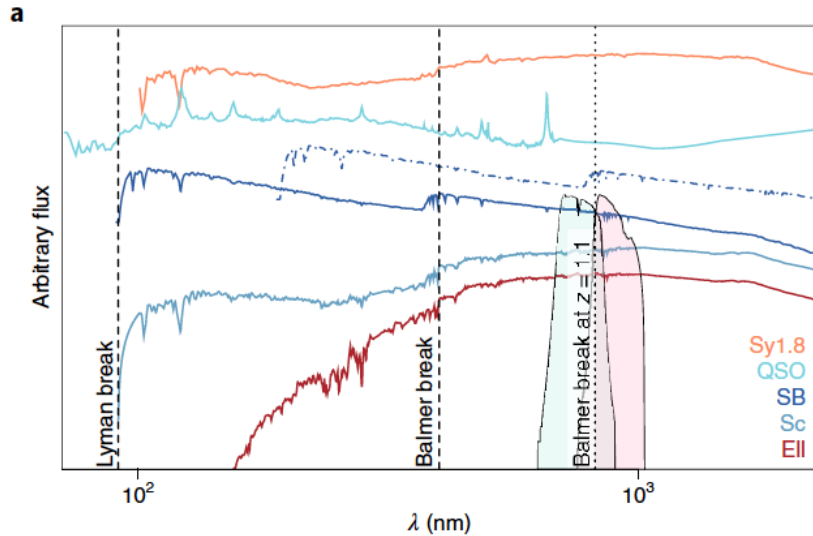
Euclid. I. Overview of Euclid mission 2024



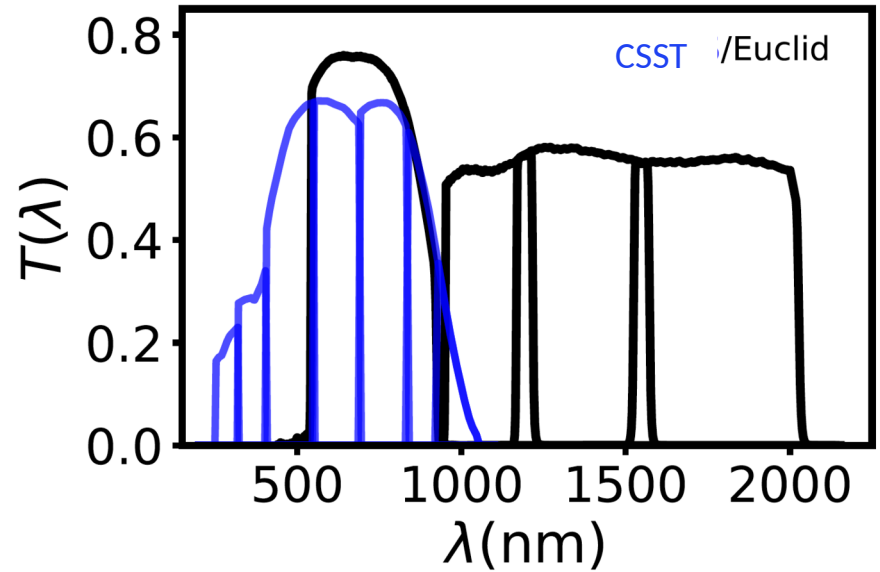
Gong et al. 2019

$z_{\text{med}} \sim 0.9$ , with a long tail up to  $z \sim 3-4$   
Galaxy number density  $n_g \sim 20-30 \text{ arcmin}^{-2}$

Photo-z measurements: redshifted SED features  $\rightarrow$  multiband photometry  
Band coverage and filters are key factors affecting the photo-z accuracy



Salvato et al. 2019



CSST and Euclid are very complementary in filters

$\rightarrow$  Utilizing the data from the two surveys can enhance the cosmological gains

$\rightarrow$  Explore the synergy of the two missions quantitatively

## Potential scientific synergies in weak lensing studies between the CSST and *Euclid* space probes

Weak Gra

fr

[ISSI/ISSI-BLI](#)

D. Z. Liu<sup>1</sup>, X. M. Meng<sup>2</sup>, X. Z. Er<sup>1</sup>, Z. H. Fan<sup>1</sup>, M. Kilbinger<sup>3</sup>, G. L. Li<sup>4,5</sup>, R. Li<sup>6,7,8</sup>, T. Schrabback<sup>9,10</sup>, D. Scognamiglio<sup>9</sup>, H. Y. Shan<sup>11,12</sup>, C. Tao<sup>13</sup>, Y. S. Ting<sup>14,15</sup>, J. Zhang<sup>16</sup>, S. H. Cheng<sup>17</sup>, S. Farrens<sup>3</sup>, L. P. Fu<sup>18</sup>, H. Hildebrandt<sup>19</sup>, X. Kang<sup>4,5</sup>, J. P. Kneib<sup>20,21</sup>, X. K. Liu<sup>1</sup>, Y. Mellier<sup>22,23</sup>, R. Nakajima<sup>9</sup>, P. Schneider<sup>9</sup>, J. L. Starck<sup>3</sup>, C. L. Wei<sup>4</sup>, A. H. Wright<sup>19</sup>, and H. Zhan<sup>2,24</sup>

(Affiliations can be found after the references)

Received 9 May 2022 / Accepted 28 October 2022

Team Members

China: [Zuhui Fa](#)  
Jun Zhang  
France: Yannick I  
Martin Ki  
Germany: Peter Sc  
Tim Schr  
Switzerland: Jean-Pa  
U.S.A.: Brice Me

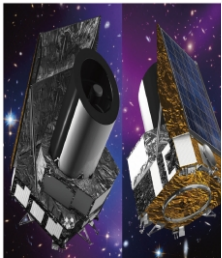
### ABSTRACT

**Aims.** With the next generation of large surveys poised to join the ranks of observational cosmology in the near future, it is important to explore their potential synergies and to maximize their scientific outcomes. In this study, we aim to investigate the complementarity of two upcoming space missions: *Euclid* and the China Space Station Telescope (CSST), both of which will be focused on weak gravitational lensing for cosmology. In particular, we analyze the photometric redshift (photo- $z$ ) measurements by combining NUV,  $u, g, r, i, z, y$  bands from CSST with the VIS,  $Y, J, H$  bands from *Euclid*, and other optical bands from the ground-based *Vera C. Rubin* Observatory Legacy Survey of Space and Time (LSST) and Dark Energy Survey. We also consider the advantages of combining the two space observational data in simplifying image deblending. For *Euclid*, weak lensing measurements use the broad optical wavelength range of 550–900 nm, for which chromatic point-spread function (PSF) effects are significant. For this purpose, the CSST narrow-band data in the optical can provide valuable information for *Euclid* to obtain more accurate PSF measurements and to calibrate the color and color-gradient biases for galaxy shear measurements.

**Methods.** We created image simulations, using the *Hubble* Deep UV data as the input catalog, for different surveys and quantified the photo- $z$  performance using the EAZY template fitting code. For the blending analyses, we employed high-resolution HST-ACS CANDELS  $F606W$  and  $F814W$  data to synthesize mock simulated data for *Euclid*, CSST, and an LSST-like survey. We analyzed the blending fraction for different cases as well as the blending effects on galaxy photometric measurements. Furthermore, we demonstrated that CSST can provide a large enough number of high signal-to-noise ratio multi-band galaxy images to calibrate the color-gradient biases for *Euclid*.

**Results.** The sky coverage of *Euclid* lies entirely within the CSST footprint. The combination of *Euclid* with the CSST data can thus be done more uniformly than with the various ground-based data that are part of the *Euclid* survey. Our studies show that by combining *Euclid* and CSST, we can reach a photo- $z$  precision of  $\sigma_{\text{NMAD}} \approx 0.04$  and an outlier fraction of  $\eta \approx 2.4\%$  at the nominal depth of the *Euclid* Wide Survey (VIS < 24.5 AB mag). For CSST, including the *Euclid*  $Y, J, H$  bands reduces the overall photo- $z$  outlier fraction from  $\sim 8.5\%$  to  $2.4\%$ . For  $z > 1$ , the improvements are even more significant. Because of the similarly high resolutions, the data combination of *Euclid* and CSST can be relatively straightforward for photometry measurements. On the other hand, to include ground-based data, sophisticated deblending utilizing priors from high-resolution space observations are required. The multi-band data from CSST are very helpful in controlling the chromatic PSF effect for *Euclid* VIS shear measurements. The color-gradient bias for *Euclid* galaxies with different bulge-to-total flux ratio at different redshifts can be well calibrated to the level of 0.1% using galaxies from the CSST deep survey.

**Key words.** dark energy – dark matter – gravitational lensing: weak – large-scale structure of Universe – surveys – telescopes



Artist view of the *Euclid* satellite

Artistic view of the E

# Photo-z: Euclid needs multiband photometry in optical bands

CSST can benefit from the infrared bands from Euclid

We performed image simulations considering CSST, Euclid and the ground-based LSST and DES → photometry → photo-z

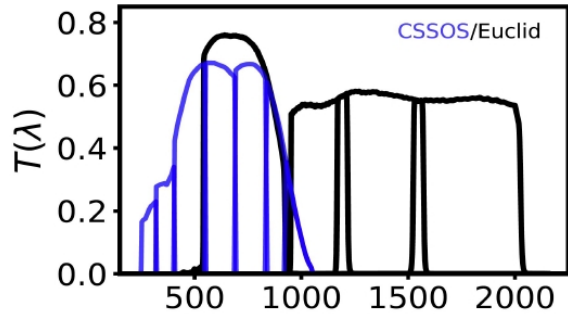


Table 1. Designed performance of CSST, *Euclid*, LSST, and DES.

Telescope/ project	Band	$\lambda_{\text{eff}}$ (Å)	$\Delta\lambda$ (FWHM) (Å)	Detection limit (mag)	Pixel scale (arcsec)	PSF size (arcsec)
CSST <sup>(a)</sup>	NUV	2880	694	25.4		0.135
	<i>u</i>	3726	866	25.4		0.135
	<i>g</i>	4734	1455	26.3		0.135
	<i>r</i>	6107	1417	26.0	0.074	0.135
	<i>i</i>	7548	1465	25.9		0.145
	<i>z</i>	8975	1082	25.2		0.165
	<i>y</i>	9606	542	24.4		0.165
<i>Euclid</i> <sup>(b)</sup>	VIS	6726	3699	24.5	0.1	0.18
	<i>Y</i>	10678	2665	24.0	0.3	0.62
	<i>J</i>	13333	4052	24.0	0.3	0.63
	<i>H</i>	17328	5023	24.0	0.3	0.70
LSST <sup>(c)</sup>	<i>u</i>	3734	623	26.1		0.81
	<i>g</i>	4731	1427	27.4		0.77
	<i>r</i>	6139	1359	27.5		0.73
	<i>i</i>	7487	1247	26.8	0.2	0.69
	<i>z</i>	8671	1022	26.1		0.68
	<i>y</i>	9677	855	24.9		0.71
DES <sup>(d)</sup>	<i>g</i>	4734	1295	24.7		1.11
	<i>r</i>	6342	1485	24.4		0.95
	<i>i</i>	7748	1480	23.8	0.263	0.88
	<i>z</i>	9139	1475	23.1		0.83
	<i>y</i>	9880	660	21.7		0.90

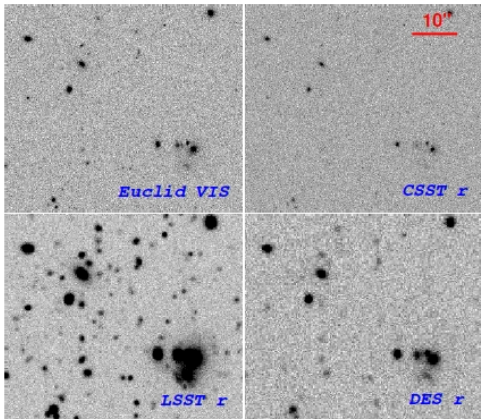


Fig. 2. Example of simulated images for *Euclid* VIS-band (upper left), CSST *r*-band (upper right), LSST-like *r*-band (lower left), and DES-like *r*-band (lower right), respectively.



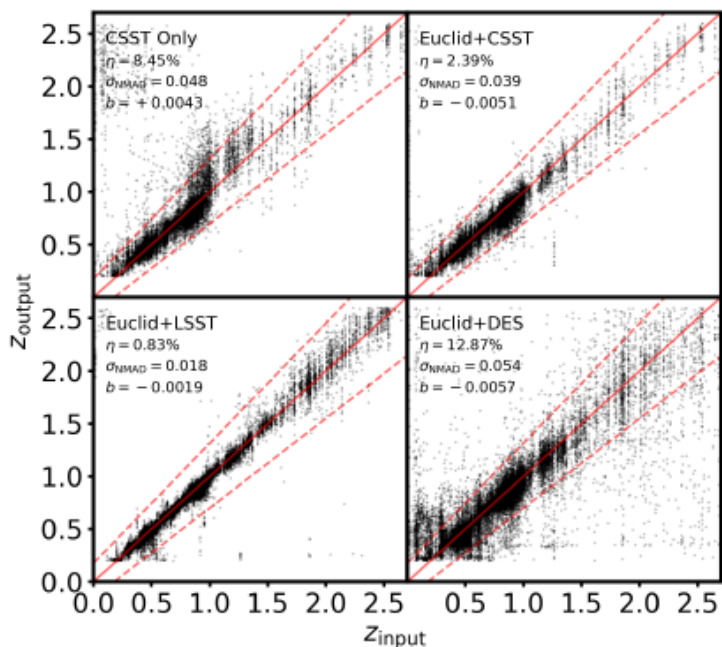
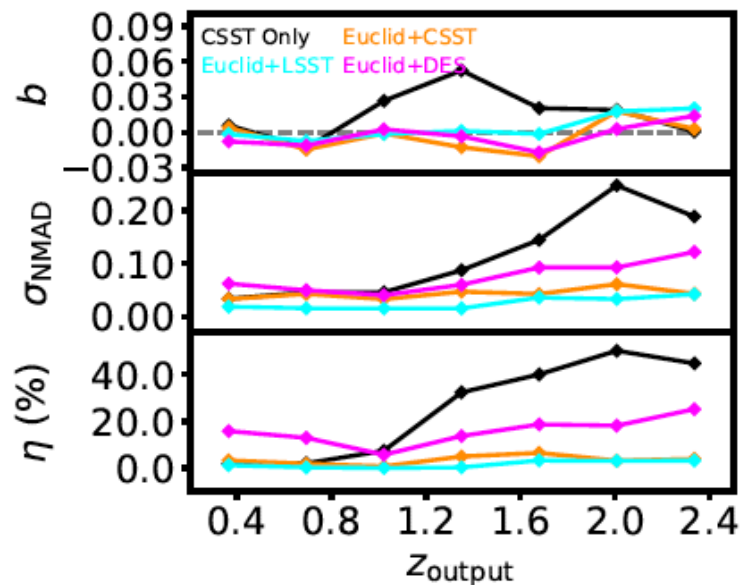
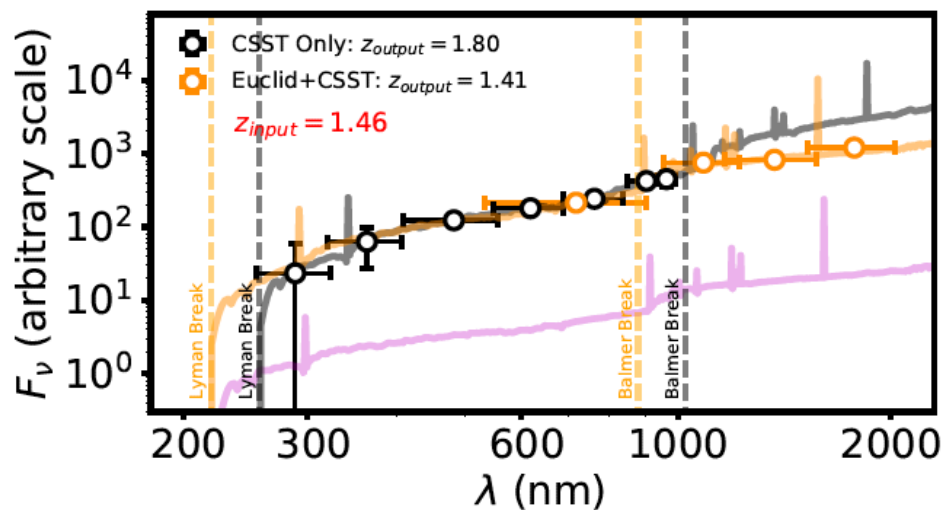


Table 2. Photo- $z$  statistics in different cases.

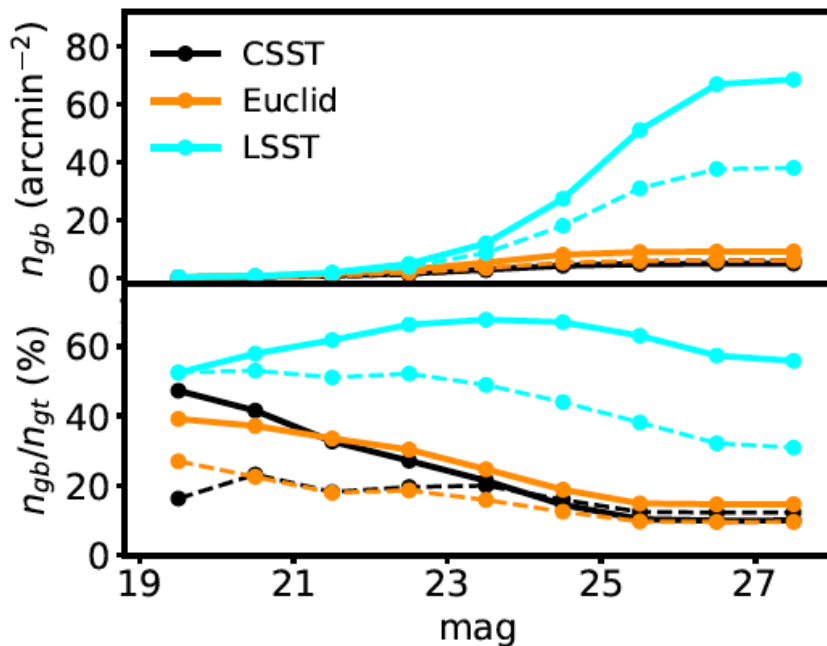
Combination	Bias	$\sigma_{\text{NMAD}}$	$\eta$
CSST-only	+0.0043	0.048	8.45%
<i>Euclid</i> +CSST	-0.0051	0.039	2.39%
<i>Euclid</i> +LSST-like	-0.0019	0.018	0.83%
<i>Euclid</i> +DES-like	-0.0057	0.054	12.87%



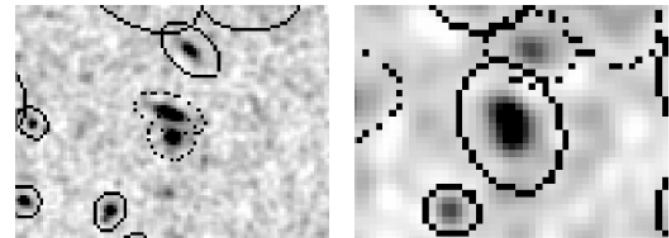
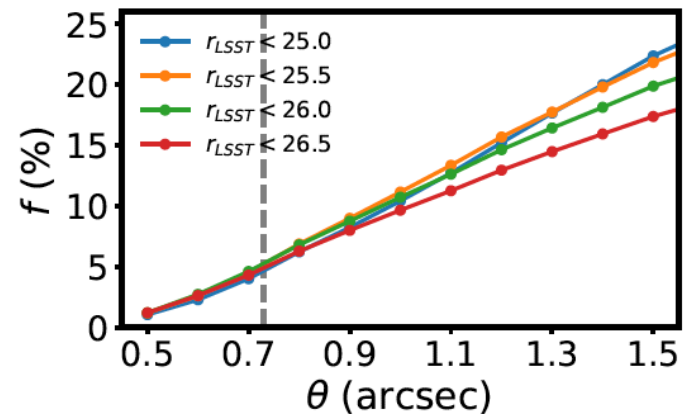
Blending problem: With the increase of depth, the problem of galaxy blending becomes increasingly troublesome, particularly for ground-based observations

→ Combine data from CSST and Euclid would be more straightforward than combining ground-based data and Euclid; also can be done uniformly over the whole survey areas.

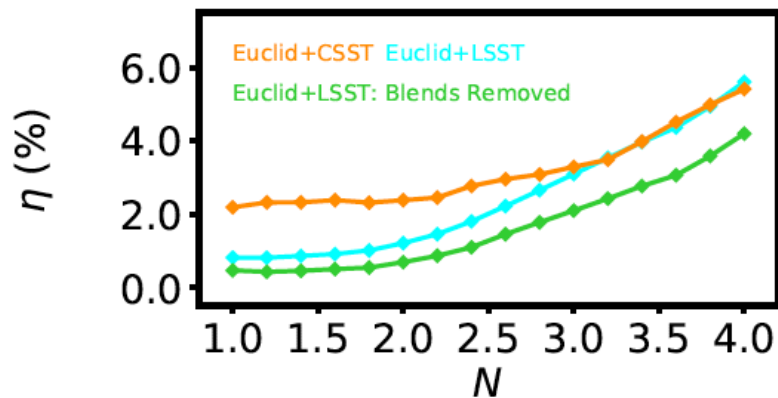
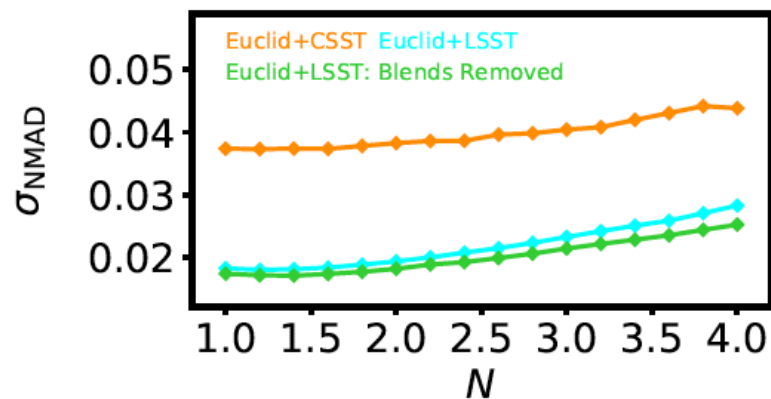
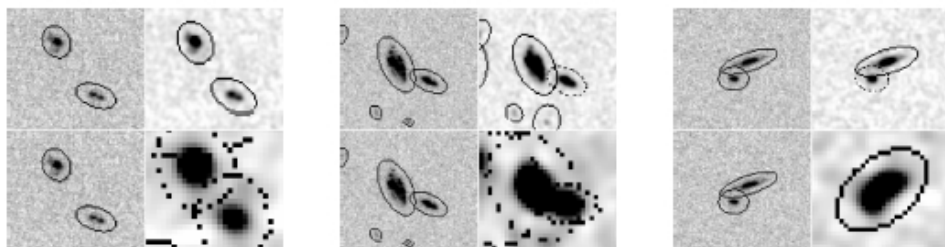
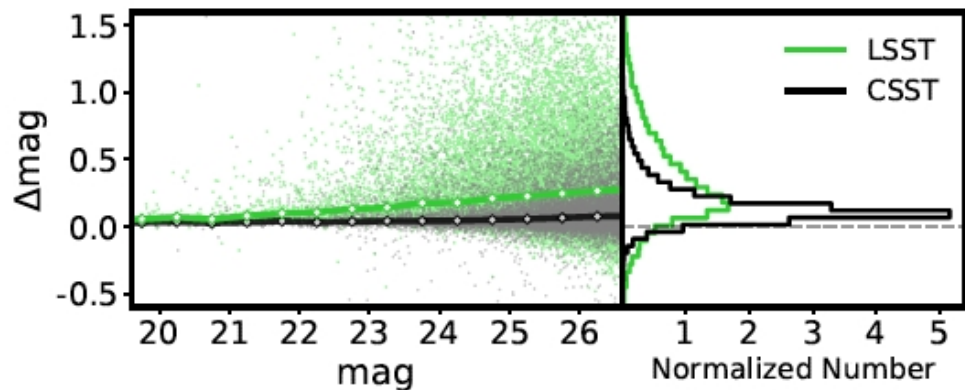
Blending fraction



Total blends



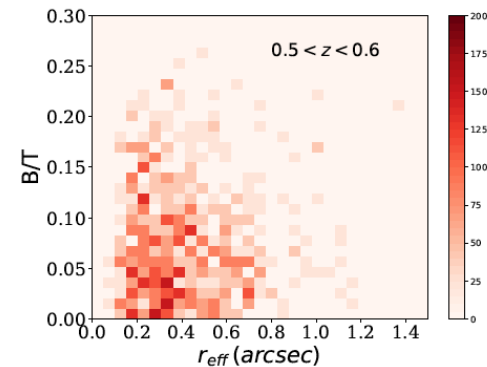
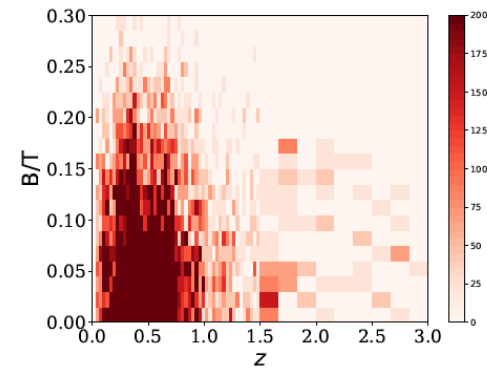
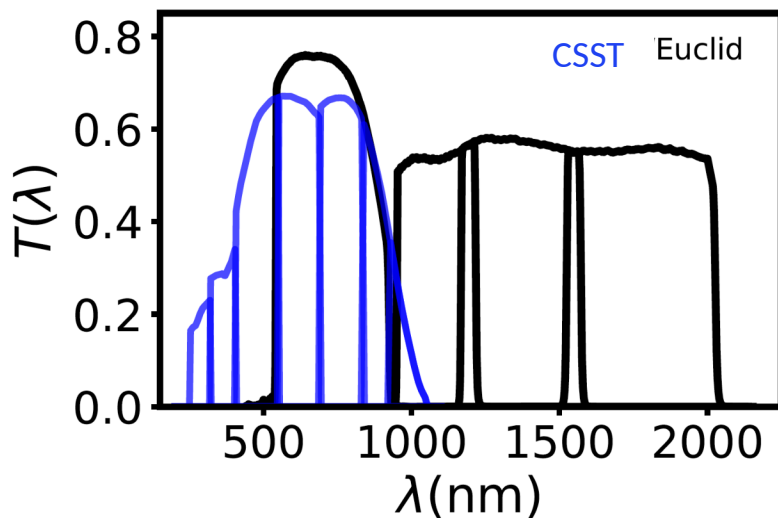
# The impact on photometry and photo-z from blending



## PSF chromaticity

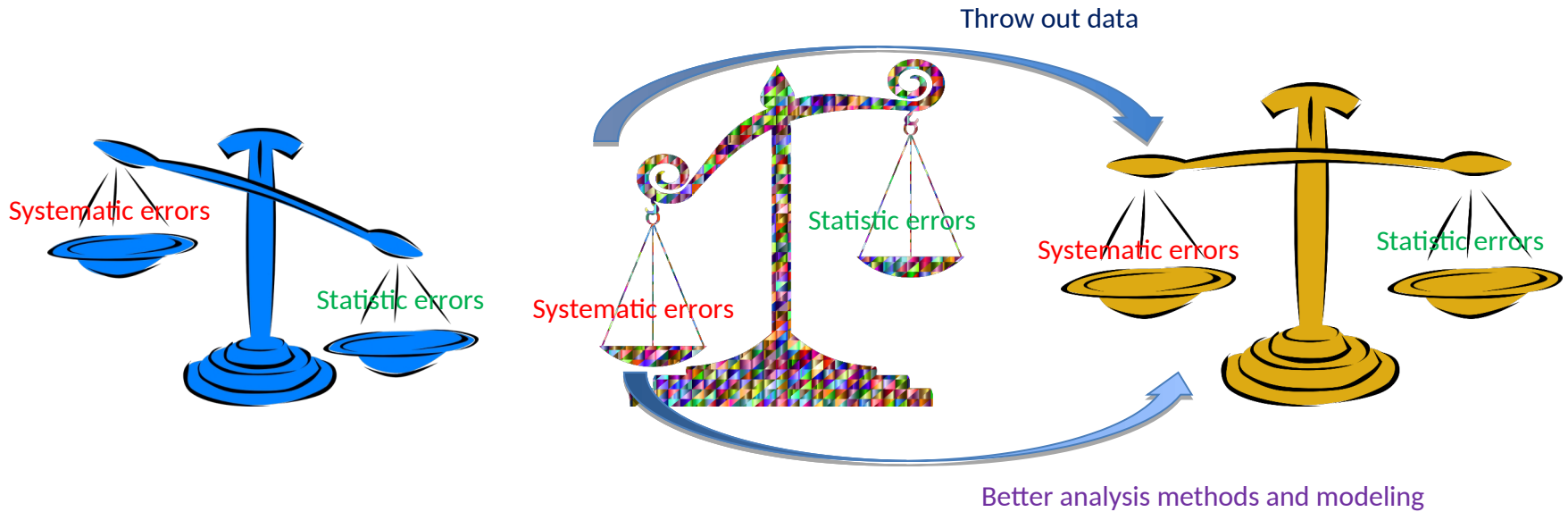
- PSF is wavelength dependent
- stars and galaxies have different SEDs
- the extrapolation of PSF measured from stars to galaxies can have biases, especially for Euclid with the broad VIS band
- galaxies have color gradients  $\rightarrow$  further biases

CSST can provide enough number of high S/N >50 narrower bands data for Euclid calibration



- **Summary**

- WL peak steepness statistics hold great potential – constrain halo density profile  
-- baryonic physics / dark matter properties



WL peak height + steepness statistics

→ constrain cosmological and astrophysical information simultaneously

- CSST and Euclid have common science objectives
  - Largely overlapped sky coverage and similarly high spatial resolutions
  - Complementary filters
  - Utilizing the data from the two surveys

- \* increase photo-z accuracy
  - reduce the outlier fraction by about a factor of 3 comparing to CSST-only case
- \* advantageous over combining with ground-based data
  - blending is much less significant
  - data can be combined uniformly over the whole survey areas
- \* control color effects on shear measurements for Euclid

Combination	Bias	$\sigma_{\text{NMAD}}$	$\eta$
CSST-only	+0.0043	0.048	8.45%
<i>Euclid</i> +CSST	-0.0051	0.039	2.39%
<i>Euclid</i> +LSST-like	-0.0019	0.018	0.83%
<i>Euclid</i> +DES-like	-0.0057	0.054	12.87%

*Thank you*